AIAA JOURNAL
Vol. 42, No. 12, December 2004

Structural Design Optimization of Shallow Frame Structures Undergoing Large Deflections

R. Sedaghati*
Concordia University, Montreal, Quebec H3G 1M8, Canada
and
A. Suleman†
University of Victoria, Victoria, British Columbia V8W 3P6, Canada

An optimization algorithm for structural design against instability is developed for shallow beam structures undergoing large deflections. The algorithm is based on the maximization of the limit load under specified volume constraint. The analysis for obtaining the limit load involves coupling of axial and bending deformations and is based on the nonlinear finite element analysis using the displacement control technique. The optimization is carried out using both the sequential-quadratic-programming (SQP) and optimality-criterion (OC) techniques, and the results are compared. For the SQP technique, the sensitivity derivatives of the critical load factor are calculated using the adjoint method based on the information obtained from the nonlinear buckling analysis. A shallow plane arch illustrates the structural design optimization methodology, and the results are compared with those in the literature. It is shown that a design based on the generalized eigenvalue problem (linear buckling) gives an optimum limit load less than the initial limit load, whereas the optimization using the nonlinear buckling analysis obtains a larger value for the optimum limit load compared to the initial limit load. It has also been demonstrated that the optimum results obtained using OC technique are in good agreement with those obtained through SQP technique. However, the computational time for the OC is significantly lower than that of SQP, which requires search techniques and sensitivity of the limit load for its successful completion and termination.

I. Introduction

GENERALLY, in design optimization problems for system buckling the design variables are selected so as to maximize the system-buckling load while keeping the volume constant. In the dual problem, the design variables are selected so as to minimize the volume of the structure while guarding against the buckling load. In this paper, this duality is addressed and investigated.

In several reported investigations[1–7] the system stability requirement has been posed as a linear buckling analysis. Such an analysis is restricted to small rotations and equilibrium in the initial state. Linear buckling reduces to the solution of a generalized eigenvalue problem for the buckling loads (bifurcation point). This definition of system stability for some flexible structures might not be conservative enough because the nonlinear behavior of the structure will result in large changes in the geometry of the structure and can play a dominant role in the control of such structures. For this reason, a nonlinear buckling analysis should be undertaken to find the more conservative buckling loads (limit point). Furthermore, in optimization of structures undergoing large deflections, finding the exact limit load is critical in order to define the objective function in the direct problem and the constraint in its dual problem.

In the past works, finite element analysis based on a load control technique[8–12] has been used to trace the nonlinear load-deflection curve in order to determine the limit load. However, the load control techniques fail as the load approaches the buckling load or requires extremely small increments to carry out the analysis. Several other procedures have been used by researchers[13–15] to overcome this difficulty. Zienkiewicz[13] has suggested a form of the displacement control method. Haisler et al.[14] have used it by partitioning the stiffness matrix. Helpful simplifications to the displacement control method have also been made in the paper by Batoz and Dhatt,[15] where one of the displacement components is incremented at each time step and an iterative process is followed.

Khot,[8] Kamat and coworkers[9–11] and Choi and Park[12] demonstrated the importance of geometrical nonlinearity in optimal design of nonlinear structural systems against instability. Sedaghati and coworkers[16–18] incorporated the displacement control technique proposed by Batoz and Dhatt[15] as an analyzer in the optimum design of truss and beam structures undergoing large deflections subject to the system stability constraint. More recently, Valido and Cardoso[19,20] have performed extensive investigation on the design sensitivity and optimal design of geometrically nonlinear composite structures.

In this study, the nonlinear buckling analysis based on the displacement control method is extended to capture the limit load for shallow frame structures (ratio of apex height to the span is less than 0.1). Two optimization methods [optimality criterion and sequential quadratic programming (SQP)] are used. The optimality algorithm presented in this study uses recurrence relation based on the uniform strain energy density distribution in the structure.[11,16] In the SQP technique the sensitivity derivatives of the critical load parameter are obtained with respect to the design variables (cross-sectional areas of the elements of the discretized model of the structure).

The calculation of the derivatives of the limit load with respect to the cross-sectional areas using finite difference might not be appropriate because of the truncation and condition errors.[21] Kamat[11] has obtained the sensitivity derivatives of the critical load parameter using implicit differentiation of equilibrium equations and the Hessian of the total potential energy, making it computationally expensive. Mroz and Haftka[22] have also addressed the sensitivity of critical load using the eigenmodes in the critical state.

In this work, the sensitivity derivatives of the limit load parameter with respect to the design variables are obtained using the adjoint method[21] based on the information obtained from the nonlinear buckling analysis.

Presented as Paper 2002-5527 at the AIAA/ISSMO 9th Symposium on Multidisciplinary Analysis and Optimization, Atlanta, GA, 4–6 September 2002; received 1 October 2003; revision received 9 June 2004; accepted for publication 9 June 2004. Copyright © 2004 by the American Institute of Aeronautics and Astronautics, Inc. All rights reserved. Copies of this paper may be made for personal or internal use, on condition that the copier pay the $10.00 per-copy fee to the Copyright Clearance Center, Inc., 222 Rosewood Drive, Danvers, MA 01923; include the code 0001-1452/04 $10.00 in correspondence with the CCC.

*Assistant Professor, Department of Mechanical and Industrial Engineering; sedagha@alcor.concordia.ca. Member AIAA.
†Associate Professor, Department of Mechanical Engineering; suleman@uvic.ca. Associate Fellow AIAA.

In the following sections, a short description of the nonlinear analysis used in the algorithm is presented. This is followed by a description of the recurrence relation used in the optimality criterion, SQP algorithms, and the derivation of the sensitivity derivatives of the limit load parameter with respect to the cross-sectional areas. To demonstrate the application of the proposed methodology, a shallow arch is optimized using both the nonlinear and the linear buckling analyses.

II. Nonlinear Analysis

In the presence of large deflections, geometrical nonlinearity becomes important. In such cases, although the strains are small and the material behaves linearly, the response of the structure becomes nonlinear as a result of finite rotations and displacements. It is therefore necessary to write the joint equilibrium in terms of the final geometry of the structure. In the case of large displacements, the strain-displacement relationships include nonlinear terms. Considering these terms and using the principle of virtual work, the system stiffness matrix can be obtained and written as

$$\boldsymbol{K} = \boldsymbol{K}_E + \boldsymbol{K}_G \tag{1}$$

where $\boldsymbol{K}$ is the system tangent stiffness matrix, $\boldsymbol{K}_E$ is the system linear elastic stiffness matrix, and $\boldsymbol{K}_G$ is the system geometric stiffness matrix. The matrix $\boldsymbol{K}_G$ is associated with the changes in the geometry of the structure. These matrices are obtained by the assemblage of the element linear elastic and geometric stiffness matrices in the global coordinates.

To derive the incremental finite element equations, it is assumed that the equilibrium configuration at a load level is known and the configuration at a slightly higher load level is to be determined. Using the fully Newton–Raphson iterative method, these equations can be written[23] as

$$^{t+\Delta t}\boldsymbol{K}^{(k-1)}\Delta\boldsymbol{U}^{(k)} = \Delta\boldsymbol{P}^{(k-1)} = {}^{t+\Delta t}\alpha^{(k)}\boldsymbol{P}_{\text{ref}} - {}^{t+\Delta t}\boldsymbol{P}'^{(k-1)}$$

$$^{t+\Delta t}\boldsymbol{U}^{(k)} = {}^{t+\Delta t}\boldsymbol{U}^{(k-1)} + \Delta\boldsymbol{U}^{(k)} \tag{2}$$

with the initial conditions

$$^{t+\Delta t}\boldsymbol{U}^{(0)} = {}^{t}\boldsymbol{U}, \qquad ^{t+\Delta t}\boldsymbol{K}^{(0)} = {}^{t}\boldsymbol{K}, \qquad ^{t+\Delta t}\boldsymbol{P}'^{(0)} = {}^{t}\boldsymbol{P}' \tag{3}$$

where k is the iteration number, $^{t+\Delta t}\boldsymbol{K}$ is the tangent stiffness matrix at time step $t+\Delta t$, $^{t+\Delta t}\boldsymbol{P}'^{(k-1)}$ is the vector of the nodal resultant member forces at time step $t+\Delta t$, $\boldsymbol{P}_{\text{ref}}$ is a given reference load, $^{t+\Delta t}\alpha$ is a load factor parameter to denote the external load at time step $t+\Delta t$, $\Delta\boldsymbol{P}$ is the out-of-balance force, $\Delta\boldsymbol{U}$ is the vector of increments in nodal displacements and $^{t+\Delta t}\boldsymbol{U}$ is the vector of nodal displacement at time step $t+\Delta t$. The out-of-balance load vector $\Delta\boldsymbol{P}$ corresponds to a load vector that is not yet balanced by element forces, and hence an increment in the nodal displacements is required. This updating of the nodal displacements in the iteration is continued until the out-of-balance loads and incremental displacements are small. To guarantee that both out-of-balance loads and incremental displacements are small, the energy convergence criteria,[23] which is a multiplication of out-of-balance force and incremental displacement, has been used in this analysis. An energy convergence tolerance of $\varepsilon_E = 10^{-6}$ has been used in this work. Increment in load or displacement is conventionally represented as an evolution in time t. The problem is of course static, and t simply denotes incremental steps in the solution.

To solve Eq. (2), the displacement control technique from Batoz and Dhatt[15] has been employed. According to this technique, instead of varying the load parameter as we do in the load control method, a nodal displacement component (for example the qth component of $^{t}\boldsymbol{U}$) is incremented by ΔU_q at each time step. Also, during each time step this component is constrained to be fixed. In other words,

$$^{t+\Delta t}U_q = {}^{t}\boldsymbol{U}_q + \Delta U_q \tag{4}$$

$$\Delta U_q^{(k)} = 0 \tag{5}$$

The constraint Eq. (5) can be directly incorporated into the original system of equations given by Eq. (2). However, this results in a modified stiffness matrix, which is not symmetric and banded any more. To overcome this problem, Eq. (2) is rewritten as

$$^{t+\Delta t}\boldsymbol{K}^{(k-1)}\left[\Delta\boldsymbol{U}^{I(k)} \,\middle|\, \Delta\boldsymbol{U}^{II(k)}\right] = \Delta\boldsymbol{P}^{(k-1)}$$

$$= {}^{t+\Delta t}\alpha^{(k)}\boldsymbol{P}_{\text{ref}} - {}^{t+\Delta t}\boldsymbol{P}'^{(k-1)} \tag{6}$$

where $\Delta\boldsymbol{U}^{I(k)}$ and $\Delta\boldsymbol{U}^{II(k)}$ can be obtained relative to $\boldsymbol{P}_{\text{ref}}$ and $^{t+\Delta t}\boldsymbol{P}'^{(k-1)}$ in each iteration using the following equations[15]:

$$^{t+\Delta t}\boldsymbol{K}^{(k-1)}\Delta\boldsymbol{U}^{I(k)} = \boldsymbol{P}_{\text{ref}}, \qquad ^{t+\Delta t}\boldsymbol{K}^{(k-1)}\Delta\boldsymbol{U}^{II(k)} = -{}^{t+\Delta t}\boldsymbol{P}'^{(k-1)} \tag{7}$$

Now, $\Delta\boldsymbol{U}^{(k)}$ can be expressed as

$$\Delta\boldsymbol{U}^{(k)} = {}^{t+\Delta t}\alpha^{(k)}\Delta U^{I(k)} + \Delta\boldsymbol{U}^{II(k)} \tag{8}$$

Writing Eq. (8) for the qth component of $^{t}\boldsymbol{U}$, we obtain

$$\Delta U_q^{(k)} = {}^{t+\Delta t}\alpha^{(k)}\Delta U_q^{I(k)} + \Delta U_q^{II(k)} \tag{9}$$

Substituting Eq. (5) into Eq. (9) gives

$$^{t+\Delta t}\alpha^{(k)} = -\frac{\Delta U_q^{I(k)}}{\Delta U_q^{II(k)}} \tag{10}$$

Having obtained the load parameter from Eq. (10), other nodal displacement components can be updated using Eq. (8). The iterative process described by Eqs. (7–10) is continued until convergence criteria is met (i.e., the new equilibrium position is found). Then, the qth component of $^{t}\boldsymbol{U}$ is incremented, and the new time step is started. During each time step, the total displacement vector is decomposed into a rigid body and a strain-producing component. Removing the rigid-body component before performing the element calculation, the remaining deformational displacement is small enough to justify the use of conventional beam element. Using this procedure known as corotational or convected coordinate approach,[24,25] an arbitrary large rotation can be obtained.

The displacement control method is useful to trace the postbuckling path. However, it does not yield the limit load factor. To obtain the optimum design of a structure for limit load, one needs to obtain the exact value of the limit load. Taking very small increments in the controlling displacement component, the limit load parameter can be approximated by the largest load parameter obtained. However, the solution obtained is sensitive to the displacement increment employed, and the cost of the solution is prohibitive. In this work, the limit load parameter is obtained by incrementing the controlling displacement component until a decrease in the load parameter is observed and performing a quadratic fit through the points a, b, c that trap the maximum point as shown in Fig. 1. By comparing the largest load, point b, and the maximum load obtained from the quadratic fit, the controlling displacement component has been modified until the increment between these two loads is within a desired tolerance. The foregoing procedure has been successfully implemented and the limit load parameter α_{cr} (the load parameter at the limit point) has been obtained with minimum computational effort.

In this paper it has been assumed that the structure is shallow and symmetric so that it exhibits limit load type of instability caused by symmetric mode. (No bifurcation type of instability or asymmetric mode occurs.) Thus, if the controlling displacement is incremented along the symmetry axis (y axis in the illustrative example), the limit load and its sensitivity can be obtained efficiently and accurately using displacement control technique just explained.

The linear elastic stiffness matrix $\boldsymbol{k}_E$ does not depend on the geometry of the structure and can be found in any finite element textbook. For a beam element as shown in Fig. 2, the element geometric stiffness matrix in local coordinates $\boldsymbol{k}_G$ can be shown as[26]

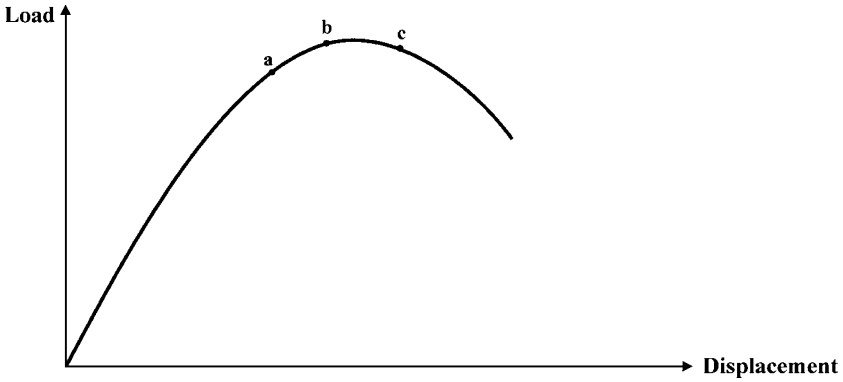

Fig. 1 Load-deflection curve and the points trapping the pick load.

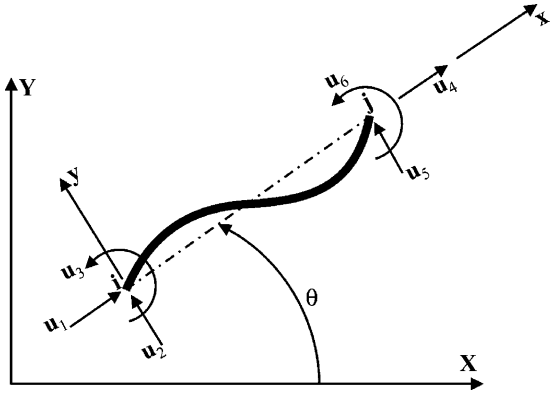

Fig. 2 Beam element with positive displacements in local axis.

The preceding matrices are defined in local axis (x, y) and can be transformed to the global coordinates (X, Y) using the rotation matrix $\boldsymbol{R}$. For the beam element, the rotation matrix is

$$\boldsymbol{R} = \begin{bmatrix} Rot & 0 \\ 0 & Rot \end{bmatrix}, \qquad Rot = \begin{bmatrix} l_x & l_y & 0 \\ -l_y & l_x & 0 \\ 0 & 0 & 1 \end{bmatrix} \tag{13}$$

where

$$l_x = \cos\theta = (X_j - X_i)/L, \qquad l_y = \sin\theta = (Y_j - Y_i)/L \tag{14}$$

are direction cosines and X_i, Y_i and X_j, Y_j are nodal coordinates at the end i and j, respectively.

Matrix $\boldsymbol{k}_\sigma$ has been obtained with a few assumptions from the matrix $\boldsymbol{k}_D$. Thus, geometric stiffness matrix $\boldsymbol{k}_D$ is more accurate than the conventional stress stiffness matrix $\boldsymbol{k}_\sigma$. In this study the geometric stiffness matrix $\boldsymbol{k}_D$ has been used in both linear and nonlinear buckling analysis.

$$\boldsymbol{k}_G = \boldsymbol{k}_D(\boldsymbol{u}) = (AE/L^2) \times \begin{bmatrix} 3(u_4-u_1) & & & \text{SYM} & & \\ \frac{-6(u_2-u_5)}{5} - \frac{L(u_3+u_6)}{10} & \frac{6(u_4-u_1)}{5} & & & & \\ \frac{-L(u_2-u_5)}{10} - \frac{L^2(4u_3-u_6)}{30} & \frac{L(u_4-u_1)}{10} & \frac{2L^2(u_4-u_1)}{15} & 3(u_4-u_1) & \text{SYM} & \\ -3(u_4-u_1) & \frac{6(u_2-u_5)}{5} + \frac{L(u_3-u_6)}{10} & \frac{L(u_2-u_5)}{10} + L^2(4u_3-u_6) & \frac{-6(u_2-u_5)}{5} - \frac{L(u_3-u_6)}{10} & \frac{6(u_4-u_1)}{5} & \\ \frac{6(u_2-u_5)}{5} + \frac{L(u_3+u_6)}{10} & \frac{-6(u_4-u_1)}{5} & \frac{-L(u_4-u_1)}{10} & \frac{L(u_2-u_5)}{10} - \frac{L^2(u_3-4u_6)}{30} & \frac{-L(u_4-u_1)}{10} & \frac{2L^2(u_4-u_1)}{15} \\ -\frac{L(u_2-u_5)}{10} + \frac{L^2(u_3-4u_6)}{30} & \frac{L(u_4-u_1)}{10} & \frac{-L^2(u_4-u_1)}{30} & & & \end{bmatrix} \tag{11}$$

where the displacements along the local x and y axis and the rotation about the local z axis at the end i are u_1, u_2, and u_3 respectively, and those at the end j are u_3, u_4, and u_6.

The matrix $\boldsymbol{k}_D$ is called displacement geometric stiffness matrix and depends on nodal displacement vector $\boldsymbol{u}$. Assuming that the nodal transverse displacements u_2, u_5 and nodal rotational displacements u_3, u_6 are sufficiently small, and considering that the quantity $AE[(u_4-u_1)/L]$ is equal to the axial force F and AE is much larger than F, the conventional element stress stiffness matrix $\boldsymbol{k}_\sigma$ (depending on the element forces) can be derived from the matrix $\boldsymbol{k}_D$:

$$\boldsymbol{k}_G = \boldsymbol{k}_\sigma = \frac{F}{30L} \begin{bmatrix} 30 & & & & & \\ 0 & 36 & & & \text{SYM} & \\ 0 & 3L & 4L^2 & & & \\ -30 & 0 & 0 & 30 & & \\ 0 & -36 & -3L & 0 & 36 & \\ 0 & 3L & -L^2 & 0 & -3L & 4L^2 \end{bmatrix} \tag{12}$$

III. Optimization Algorithms

The optimization problem can be defined as follows: Find the vector of element cross-sectional areas $\boldsymbol{A}$ (design variables):

Maximize the limit load factor

$$\alpha_{\text{cr}}(\boldsymbol{A})$$

Subject to

$$V = \boldsymbol{A}^T\boldsymbol{L} - \bar{V} = 0, \qquad \boldsymbol{A}_l - \boldsymbol{A} \le 0 \tag{15}$$

where $\boldsymbol{L}$ is the vector of elemental length, V and $\bar{V}$ are the total volume and the specified total volume of the structure, α_{cr} is the

limit load factor and the specified limit load factor, respectively, and $\boldsymbol{A}_l$ is the lower bound of the design variable vector $\boldsymbol{A}$.

In this study, the optimization methods based on the optimality-criterion (OC) and SQP technique have been used, and the results are compared.

A. Optimality Criteria

For the frame type of structures the optimality criteria can be stated as[11,18]

$$\lambda\hat{\Pi}_i = \lambda\left[\left(\Pi_i^s + \Pi_i^b\right)\Big/ V_i\right] = 1 \qquad \text{for} \qquad i = 1, 2, \ldots, n \quad (16)$$

where $\hat{\Pi}_i$, Π_i^s, Π_i^b are the total stain energy density, strain energy caused by stretching, and the strain energy caused by bending, all calculated at the limit point, respectively, and V_i is the volume of the ith element, λ is the Lagrange multiplier related to the equality constraint, and n is the number of beam elements. To obtain a design satisfying the optimality criterion in Eq. (16), a recurrence procedure that evolves design is used. This consists of changing the design variables by using the recurrence relation after determining the limit load factor and the associated deformed shape of the structure. A simple and efficient form of the recurrence relation can be expressed by multiplying both sides of Eq. (16) by $(A_i)^\beta$ and taking its βth root as

$$A_i^{v+1} = A_i^v\left(\lambda\hat{\Pi}_i\right)_v^{1/\beta} \quad (17)$$

where A_i^v and A_i^{v+1} are the cross-sectional area of the ith element at the vth and $(v+1)$th iteration, respectively. The step size parameter β controls the convergence rate and can be changed by assigning appropriate values.

To use Eq. (17), it is required to know the value of the Lagrange multiplier λ. At the optimal design, λ will satisfy Eq. (16). For nonoptimal design it is desired to obtain a value of λ that most closely satisfies this equation. In nonoptimal design, consider a residual Res defined as

$$Res_i = 1 - \lambda\hat{\Pi}_i \quad (18)$$

Now, λ is taken as the value that minimizes the sum of the squares of the residuals, that is, the value for which

$$\frac{\mathrm{d}}{\mathrm{d}\lambda}\left[\sum_{i=1}^{n} Res_i^2\right] = 0 \quad (19)$$

Equation (19) results in the following closed-form solution for the value of λ:

$$\lambda = \sum_{i=1}^{n}\hat{\Pi}_i \Bigg/ \sum_{i=1}^{n}\hat{\Pi}_i^2 \quad (20)$$

Substituting Eq. (20) into Eq. (17), we finally obtain the following recurrence relation for updating the design variables:

$$A_i^{v+1} = A_i^v\left(\left[\sum_{i=1}^{n}\hat{\Pi}_i \Bigg/ \sum_{i=1}^{n}\hat{\Pi}_i^2\right]\hat{\Pi}_i\right)_v^{1/\beta} \quad (21)$$

According to the optimization problem stated in the Eq. (15), the structural volume V must be equal to the specified volume $\bar{V}$. If this condition is satisfied at the end of each iteration, then every design will be a feasible one. This can be achieved by linear scaling the design variables following the nonlinear analysis phase in the iteration cycle. The scale factor S_f can be obtained by

$$S_f = V/\bar{V} \quad (22)$$

Thus the scaled design variable $\tilde{A}_i$ can be written as

$$\tilde{A}_i = S_f A_i \quad (23)$$

The side constraints in Eq. (15) were treated as passive constraints. If the recurrence relation reduced the area of any element to a value smaller than the minimum specified, then the cross-sectional area of that element was set to the minimum size.

B. Sequential Quadratic Programming

The SQP method used in this study is based on the work by Powell.[27] The method allows you to closely mimic Newton's method for constraint optimization just as is done for unconstraint optimization. SQP is indirectly based on the solution of Karush–Kuhn–Tucker (KKT) conditions.

The MATLAB® SQP implementation[28] has been used to obtain the optimal results. In SQP method, it is required to obtain the gradient of the Lagrangian function. This gradient involves the gradient of the objective function and the constraints with respect to the design variables.

The gradient of the behavior and side constraints is relatively straightforward because they are explicitly dependent on the design variables. However, the gradient of the objective function in Eq. (15) requires the gradient of the limit load factor, which will be explained in the following section.

IV. Sensitivity of the Critical Load Factor

The approach is based on the explicit differentiation of the equilibrium equation at the limit load. Let us assume that the limit load factor has been obtained at the current design after completing the nonlinear buckling analysis using the displacement control method. Recalling Eq. (2), the equations of equilibrium of the structure at the limit load (critical sate) can be given by[2]

$$\alpha_{\mathrm{cr}}\boldsymbol{P}_{\mathrm{ref}} - \boldsymbol{P}' = 0 \quad (24)$$

The reference to time step t and iteration k are dropped here, assuming that final converged solution of the nonlinear finite element equations has been reached and the limit load factor α_{cr} has been obtained. Differentiating Eq. (24) with respect to a typical design variable A_i gives the following equation:

$$\frac{\mathrm{d}\alpha_{\mathrm{cr}}}{\mathrm{d}A_i}\boldsymbol{P}_{\mathrm{ref}} + \alpha_{\mathrm{cr}}\frac{\mathrm{d}\boldsymbol{P}_{\mathrm{ref}}}{\mathrm{d}A_i} - \frac{\mathrm{d}\boldsymbol{P}'}{\mathrm{d}A_i} = 0 \quad (25)$$

Here, the reference load $\boldsymbol{P}_{\mathrm{ref}}$ does not depend on the deformation and the design variables (dead load). Therefore its differentiation with respect to the design variables is zero. Using the chain rule,

$$\frac{\mathrm{d}\boldsymbol{P}'}{\mathrm{d}A_i} = \frac{\partial\boldsymbol{P}'}{\partial A_i} + \frac{\partial\boldsymbol{P}'}{\partial\boldsymbol{U}}\frac{\mathrm{d}\boldsymbol{U}}{\mathrm{d}A_i} \quad (26)$$

is obtained. Substituting Eq. (26) into Eq. (25) and rearranging the terms yields

$$\frac{\partial\boldsymbol{P}'}{\partial\boldsymbol{U}}\frac{\mathrm{d}\boldsymbol{U}}{\mathrm{d}A_i} = \frac{\mathrm{d}\alpha_{\mathrm{cr}}}{\mathrm{d}A_i}\boldsymbol{P}_{\mathrm{ref}} - \frac{\partial\boldsymbol{P}'}{\partial A_i} \quad (27)$$

Considering that the rate of change of the nodal internal forces with respect to the nodal displacements is equal to the tangential stiffness matrix $\boldsymbol{K}$, Eq. (27) can be written as

$$\boldsymbol{K}\frac{\mathrm{d}\boldsymbol{U}}{\mathrm{d}A_i} = \frac{\mathrm{d}\alpha_{\mathrm{cr}}}{\mathrm{d}A_i}\boldsymbol{P}_{\mathrm{ref}} - \frac{\partial\boldsymbol{P}'}{\partial A_i} \quad (28)$$

Equation (28) contains more unknowns than equations; therefore, it cannot be solved directly to obtain the sensitivity of the load factor $\mathrm{d}\alpha_{\mathrm{cr}}/\mathrm{d}A_i$. To overcome this problem, the displacement control technique strategy explained in Sec. II has been extended to solve Eq. (28).

Similar to Eq. (6), Eq. (28) can be cast to the following equation:

$$\boldsymbol{K}\left[\frac{\mathrm{d}\boldsymbol{U}^I}{\mathrm{d}A_i}\middle|\frac{\mathrm{d}\boldsymbol{U}^{II}}{\mathrm{d}A_i}\right] = \frac{\mathrm{d}\alpha_{\mathrm{cr}}}{\mathrm{d}A_i}\boldsymbol{P}_{\mathrm{ref}} - \frac{\partial\boldsymbol{P}'}{\partial A_i} \quad (29)$$

where similar to Eq. (7), $d\boldsymbol{U}^I/dA_i$ and $d\boldsymbol{U}^{II}/dA_i$ can be obtained relative to $\boldsymbol{P}_{\text{ref}}$ and $\partial\boldsymbol{P}'/\partial A_i$ in each iteration using the following equations:

$$\boldsymbol{K}\frac{d\boldsymbol{U}^I}{dA_i} = \boldsymbol{P}_{\text{ref}}, \qquad \boldsymbol{K}\frac{d\boldsymbol{U}^{II}}{dA_i} = -\frac{\partial\boldsymbol{P}'}{\partial A_i} \tag{30}$$

Now, $d\boldsymbol{U}/dA_i$ can be expressed as

$$\frac{d\boldsymbol{U}}{dA_i} = \frac{d\alpha_{\text{cr}}}{dA_i}\frac{d\boldsymbol{U}^I}{dA_i} + \frac{d\boldsymbol{U}^{II}}{dA_i} \tag{31}$$

Writing Eq. (31) for the qth component of $\boldsymbol{U}$, we obtain

$$\frac{dU_q}{dA_i} = \frac{d\alpha_{\text{cr}}}{dA_i}\frac{dU_q^I}{dA_i} + \frac{dU_q^{II}}{dA_i} \tag{32}$$

Considering Eq. (5), it is obvious that

$$\frac{dU_q}{dA_i} = 0 \tag{33}$$

Substituting Eq. (33) into Eq. (32), the sensitivity of the critical load factor can be obtained as

$$\frac{d\alpha_{\text{cr}}}{dA_i} = -\frac{dU_q^{II}}{dA_i}\Big/\frac{dU_q^I}{dA_i} \tag{34}$$

To obtain dU_q^I/dA_i and dU_q^{II}/dA_i efficiently with less computational effort, the adjoint method is used. First, an adjoint vector η is defined such that

$$\boldsymbol{K}\eta = \boldsymbol{Z} \tag{35}$$

where the vector $\boldsymbol{Z}$ is the dummy load with its qth component equal to unity so that

$$\frac{dU_q^I}{dA_i} = \boldsymbol{Z}^T\frac{d\boldsymbol{U}^I}{dA_i}, \qquad \frac{dU_q^{II}}{dA_i} = \boldsymbol{Z}^T\frac{d\boldsymbol{U}^{II}}{dA_i} \tag{36}$$

Now, substituting $d\boldsymbol{U}^I/dA_i$ and $d\boldsymbol{U}^{II}/dA_i$ from Eq. (30) and $\boldsymbol{Z}$ from Eq. (35) into Eq. (36), we finally obtain

$$\frac{dU_q^I}{dA_i} = \eta^T\boldsymbol{P}_{\text{ref}}, \qquad \frac{dU_q^{II}}{dA_i} = -\eta^T\frac{\partial\boldsymbol{P}'}{\partial A_i} \tag{37}$$

For calculating the adjoint vector η from Eq. (35), there is no need to obtain the tangent stiffness matrix $\boldsymbol{K}$ because it is available from the converged solution of the nonlinear buckling analysis (limit point). Equation (37) involves only calculation of $\partial\boldsymbol{P}'/\partial A_i$, which can be readily obtained.

Using the preceding procedure, the sensitivity of the limit load can be easily obtained with no extra computational burden in contrast to the other methods in the literature,[11,21,22] which needs implicit differentiation of equilibrium equations and the Hessian of the total potential energy or the calculation of the eigenmodes in the critical state.

V. Illustrative Example

A simply supported sinusoidal arch is investigated in this study. The arch and its finite element model are shown in Fig. 3.

The arch is modeled using 10 plane beam elements, which have equal projections in the X axis. The arch's span is 254 cm (100 in.). The Young's modulus is assumed to be $E = 6.895 \times 10^{11}$ N/m^2 (10^8 psi). The moment of inertia I of the beam elements is such that $I = aA^b$, where A is the cross-sectional area; $b = 1, 2, 3$; and a is a specified constant. For $b = 1$ and $b = 3$, the rectangular cross section with unit constant depth-variable width and variable depth-unit constant width have been considered, respectively. For $b = 2$, the solid circular cross section is selected.

The analysis of the arch for its limit load calculation involves nonlinear buckling analysis. The nonlinear buckling analysis based on the displacement control method explained in Sec. II has been implemented successfully to capture limit load as accurately as desired. The downward vertical displacement at node 6 is taken as the controlling displacement. The displacement is applied at a rate of 0.254 cm (0.1 in.) in each time step. Two arches with different apex height H have been investigated. For apex height of $H = 12.7$ cm (5 in., low-rise arch), the limit load is maximized under specified volume of 655.48 cm^3 (40 in.^{3}), whereas for $H = 25.4$ cm (10 in., intermediate-rise arch) the specified volume of 573.55 cm^3 (35 in.^{3}) is considered. The feasible initial design with cross-sectional area of 2.565 cm^2 for arch with $H = 12.7$ cm and 2.205 cm^2 for arch with $H = 25.4$ cm has been selected. The main objective is to investigate how much increase in the limit load can be gained by redistributing the cross-sectional area. The final results using the OC based on the recurrence relation in Eq. (21) are given in Table 1. It is emphasized that although no linking design variables strategy was adopted the final cross-sectional areas have been found to be exactly symmetric. Both fully geometrical nonlinear buckling analysis and linear buckling analysis (stability eigenanalyses) have been performed. The results reveal that when using the nonlinear buckling analysis an increase in limit load is achieved. This increase is greatest for the

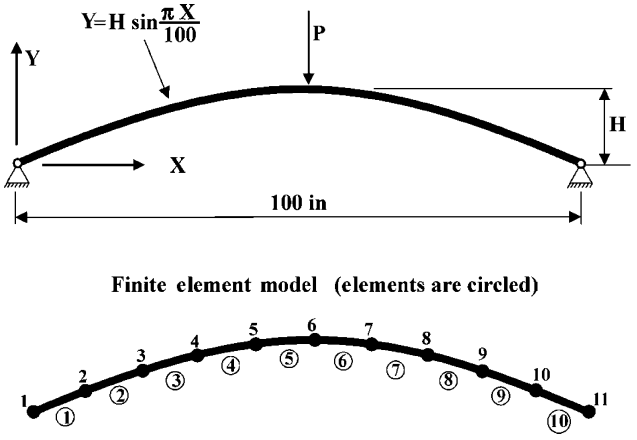

Fig. 3 Sinusoidal arch and its finite element model.

Table 1 Final design for area of cross sections (cm^2): shallow arch (OC)[a]

Parameter	Analysis	Element 1	2	3	4	5	$(P_{\text{cr}})_{\text{opt}}/(P_{\text{cr}})_{\text{initial}}$
$b = 1$	Linear	1.4316	1.7568	1.7568	2.1245	5.7813	0.8961
$H = 12.7$ cm	Nonlinear	1.8942	2.0432	2.0419	2.4168	4.4516	1.136
$b = 1$	Linear	1.1297	1.4561	1.4561	1.7606	5.3206	0.9607
$H = 25.4$ cm	Nonlinear	1.6581	1.7903	1.7877	2.0258	3.8206	1.136
$b = 2$	Linear	1.3677	1.4774	1.4774	3.0393	5.4916	0.6617
$H = 12.7$ cm	Nonlinear	2.0013	2.0019	1.8658	2.9026	4.0716	1.235
$b = 2$	Linear	1.0845	1.1458	1.1458	2.7632	4.9948	0.6587
$H = 25.4$ cm	Nonlinear	1.7323	1.7335	1.5910	2.5039	3.5168	1.236
$b = 3$	Linear	1.4890	1.4890	1.5064	3.3271	5.0400	0.5269
$H = 12.7$ cm	Nonlinear	2.1264	2.1271	1.9226	2.9329	3.7297	1.315
$b = 3$	Linear	1.2168	1.2168	1.3290	2.9206	4.4361	0.5596
$H = 25.4$ cm	Nonlinear	1.8406	1.8413	1.6464	2.5245	3.2129	1.314

[a]The areas of the elements on the other half of the arch can be found by symmetry.

Table 2 Final relative strain energy density: shallow arch (OC, nonlinear buckling)

Parameter	Element 1	2	3	4	5
$b = 1$					
$H = 12.7$ cm	0.9726	0.9621	0.9621	1.0000	0.9878
$H = 25.4$ cm	0.9435	0.9237	0.9236	1.0000	0.9782
$b = 2$					
$H = 12.7$ cm	1.0000	1.0000	0.9976	1.0000	0.9973
$H = 25.4$ cm	0.9999	0.9999	1.0000	0.9999	0.9999
$b = 3$					
$H = 12.7$ cm	1.0000	1.0000	1.0000	1.0000	1.0000
$H = 25.4$ cm	1.0000	1.0000	1.0000	1.0000	1.0000

Table 3 Final design using 20 elements: arch with $b = 1$ (OC, nonlinear buckling)

Element	Cross-sectional area $H = 12.7$ cm	$H = 25.4$ cm	Relative strain energy $H = 12.7$ cm	$H = 25.4$ cm
1	0.21244	0.1775	0.9978	0.9942
2	0.3291	0.2881	0.9979	0.9940
3	0.3809	0.3358	0.9975	0.9941
4	0.3810	0.3359	0.9975	0.9941
5	0.3567	0.3110	0.9967	0.9943
6	0.2548	0.2135	0.9950	0.9947
7	0.2252	0.1816	1.0000	0.9973
8	0.4300	0.3664	0.9978	0.9976
9	0.6204	0.5364	0.9966	0.9987
10	0.7922	0.6888	0.9956	1.0000
$(P_{cr})_{opt}/(P_{cr})_{initial}$	1.219	1.230	——	——

arch with $b = 3$. Using an arch with $b = 3$ ($H = 12.7$ or 25.4 cm), the limit load for the optimal design was increased approximately 1.314 times compared to that of the initial design.

As expected, erroneous results are obtained using the linear buckling analysis. When using the linear buckling analysis, the limit load in the final design was decreased. The final relative strain energy for nonlinear buckling analysis is given in the Table 2. The relative strain energy is nearly uniform in all cases. For the $b = 3$, in both $H = 12.7$ and 25.4 cm, the exact uniform strain energy has been obtained, indicating that the optimal solution has been obtained. For the case $b = 1$, in both $H = 12.7$ and 25.4 cm the uniform strain energy has not been obtained exactly.

To improve the uniformity of the strain energy, the number of the elements was doubled to 20 elements. As a consequence, the nonlinear buckling analysis using 20 elements was obviously found to be computationally much more expensive than that of 10 elements. The results are shown in the Table 3.

Fairly uniform strain energy was obtained for the arch modeled with 20 elements. For the arch with $b = 1$ and $H = 12.7$ cm modeled with 10 and 20 elements, the ratio of the final limit load to the initial limit load was increased from 1.136 to 1.219, respectively. Similarly for the arch with $b = 1$ and $H = 25.4$ cm modeled with 10 and 20 elements, the ratio of the final limit load to the initial limit load was increased from 1.136 to 1.230, respectively. Thus, when the uniformity of the strain energy is not satisfactory, increasing the number of the elements may help to increase the uniformity and obtaining more accurate optimal solution. The iteration history for the arch with $b = 1$ and $H = 12.7$ cm and 25.4 cm modeled with 10 and 20 elements and using nonlinear buckling analysis is shown in the Fig. 4.

In all cases, the volume of the arch in the optimum design was found to be 655.48 cm^3 for $H = 12.7$ cm and 573.55 cm^3 for $H = 25.4$ cm. For instance, for $H = 12.7$ cm and $b = 1$ the final volume was 655.484117 cm^3, or for $H = 25.4$ cm and $b = 3$ the final volume was found to be 573.547286 cm^3. This confirms that the required volume constraint was totally satisfied.

The initial and final optimum configuration of the arch for $b = 1$ with both $H = 12.7$ and 25.4 cm is shown in the Fig. 5. It is clear that the symmetry of the arch is held in the final optimum design,

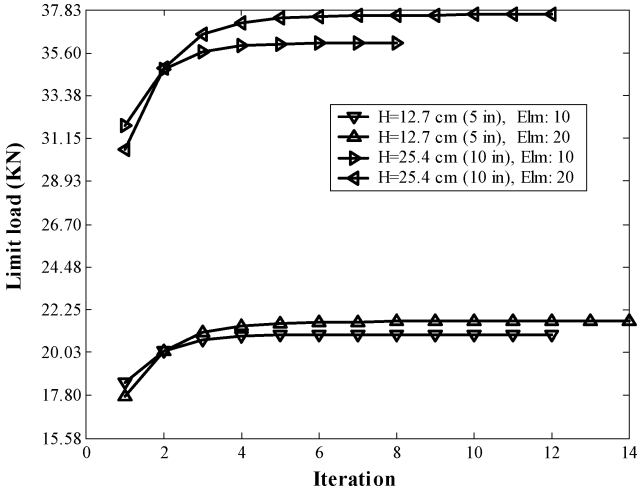

Fig. 4 Iteration history for the arch with $b = 1$ modeled with 10 and 20 elements.

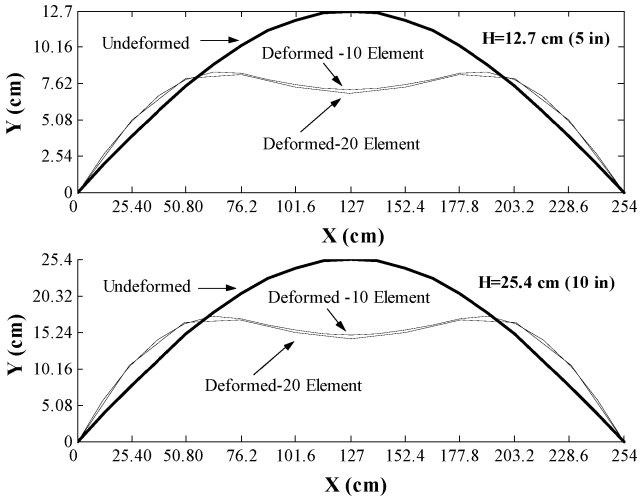

Fig. 5 Unreformed and optimal deformed configuration: shallow arch with $b = 1$.

indicating that the design is driven by the axisymmetric mode. The eigenanalysis of the optimum design (using nonlinear buckling analysis) confirms that the fundamental buckling mode is symmetric.

Finally, the optimization results obtained by the OC were compared to those obtained using the SQP technique. This method was found to be computationally much more expensive than the OC. Moreover, the possibility that the design can be cast into a region where no limit load can be determined is relatively high. The results are shown in the Table 4.

Although it was expected to obtain more accurate optimum solution using the mathematical programming technique, this turns out to be not the case for the arch with $b = 1$. The limit load ratio of 1.136 was obtained using OC, and it was found to be 1.018 using SQP. The lower limit load ratio in the SQP can be attributed to the premature termination during the optimization process. The SQP method complained that no limit load can be found in some iterations for arch with $b = 1$. Considering that the shallow arch might exhibit no distinct limit load for some area distributions, this can be interpreted that during the iteration process the design variables were updated in such a way that no limit load exists in the following iteration. For these kinds of situations, the optimization process will fail or terminate prematurely. However, for $b = 2$ and 3, the good agreement exists between the OC and SQP methods. The problem was tried with a different initial guess, and in all cases the optimum solution was found to be the same. The iteration history for OC and SQP for the arch with $H = 12.7$ and 25.4 cm using nonlinear buckling analysis are shown in the Figs. 6 and 7, respectively.

Table 4 Final designs for area of cross sections (cm^2): (SQP, nonlinear buckling)

Parameter	Element 1	2	3	4	5	$(P_{cr})_{opt.}/(P_{cr})_{initial}$
$H = 12.7$ cm (5 in.)						
$b = 1$	2.3948	2.4600	2.5652	2.6703	2.7374	1.018
$b = 2$	2.0394	2.8090	2.3097	1.9594	3.7142	1.222
$b = 3$	1.9916	2.4761	1.6529	2.9135	3.8026	1.379
$H = 25.4$ cm (10 in.)						
$b = 1$	2.0561	2.2568	2.1181	2.2948	2.3052	1.018
$b = 2$	1.5581	2.1000	1.2045	2.5439	3.6716	1.303
$b = 3$	1.7368	2.1413	1.4194	2.5026	3.2652	1.376

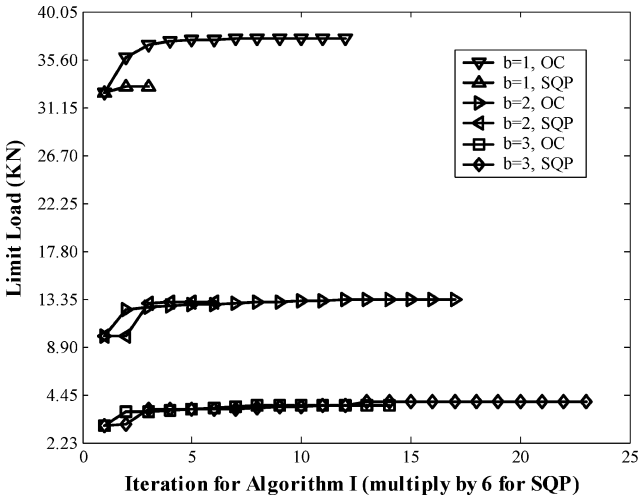

Fig. 6 Iteration history for the arch with $H = 12.7$ cm using OC and SQP.

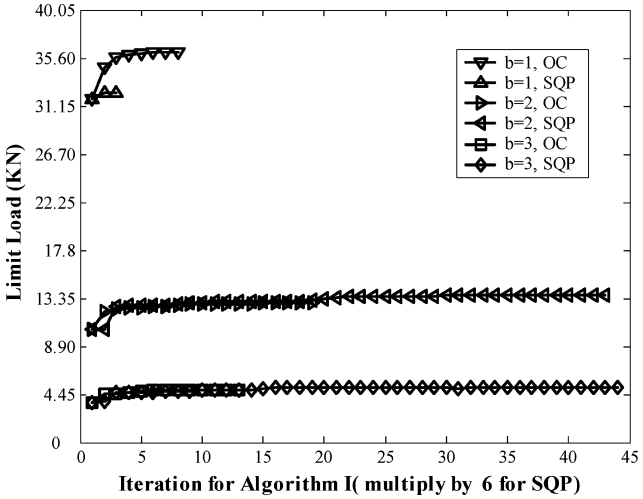

Fig. 7 Iteration history for the arch with $H = 25.4$ cm using OC and SQP.

This problem has also been addressed by Kamat.[11] The approach was based on the nonlinear analysis using the force control method. Both VMCON code, which is based on the gradient search techniques, and optimality criterion based on the maximum potential energy in optimum design were used as optimizers. The problem was addressed for just $H = 25.4$ cm, and it is mentioned that for $H = 12.7$ cm the optimization failed because no limit load was determined. For 25.4 cm, the limit load ratio for the arch with $b = 1$ (1.033 and 1.047 using VMCON and the algorithm based on the maximization of the potential energy, respectively) was lower than that found in the present investigation (1.136). For $b = 2$ and 3, the limit load ratios of 1.064 and 1.092 were obtained respectively, through maximization of the potential energy,[11] which is considerably lower than that of the current research.

Because the algorithm based on the maximum potential energy in the optimum design is naturally the same as the algorithm based on the uniform strain energy in the optimum design, the lower limit load ratio obtained in Ref. 11 can be explained by not catching accurately the limit load during the course of the optimization or not using an appropriate Lagrange multiplier formula in the relative algorithm.

VI. Conclusions

An optimization algorithm has been developed to maximize the limit load of frame structures under volume constraint. The algorithm combines the nonlinear buckling analysis using the displacement control technique as analyzer, with optimality-criterion technique based on the uniform strain energy, and mathematical-programming technique based on the sequential-programming technique, as optimizers.

It has been demonstrated that design based on the generalized eigenvalue problem (linear buckling) can exhibit erroneous results. No increase in the limit load was observed in design based on the linear stability analysis. It is concluded that in all cases, during the optimization process, a limit point type of instability exists. However, for arches or frames with high-apex-height-to-span ratio, the type of instability can change from the initial limit point to a bifurcation type at convergence or it can exhibit exclusively a bifurcation type of instability. For these types of problems, the generalized eigenvalue problem can be justified. It has also been shown that the optimum results obtained using optimality-criterion (OC) technique based on the uniform strain energy density are in good agreement with those obtained through mathematical-programming technique based on the sequential-quadratic-programming (SQP) technique. In some cases, the optimum limit load using OC is greater than that of SQP. When using a simple recurrence relation for updating the design variables in OC, the computational time for the OC is significantly lower than that of SQP, which requires search techniques and sensitivity of the limit load for its successful completion and termination.

Finally, it is concluded that catching the limit load as accurately as possible is crucial in structural optimization of the frame structures against instability. Failing to catch the limit load accurately can accumulate the errors at each iteration of the optimization procedure and can cause the design variables to be cast in a region where no limit load is available for the structure, thus causing the premature termination of the optimization procedure.

References

[1]Kiusalaas, J., "Optimal Design of Structures with Buckling Constraints," *International Journal of Solids and Structures*, Vol. 9, No. 7, 1973, pp. 863–878.

[2]Khot, N. S., Venkayya, V. B., and Berke, L., "Optimum Structural Design with Stability Constraints," *International Journal for Numerical Methods in Engineering*, Vol. 10, No. 5, 1976, pp. 1097–1114.

[3]Khot, N. S., "Nonlinear Analysis of Optimized Structure with Constraints on System Stability," *AIAA Journal*, Vol. 21, No. 8, 1983, pp. 1181–1186.

[4]Levy, R., and Perng, H. S., "Optimization for Nonlinear Stability," *Computers and Structures*, Vol. 30, No. 3, 1988, pp. 529–535.

[5]Szyskowski, W., Watson, L. G., and Fietkiewicz, B., "Bimodal Optimization of Frames for Maximum Stability," *Computers and Structures*, Vol. 32, No. 5, 1989, pp. 1093–1104.

[6]Canfield, R. A., "Design of Frames Against Buckling Using a Rayleigh Quotient Approximation," *AIAA Journal*, Vol. 31, No. 6, 1993, pp. 1144–1149.

[7]Levy, R., "Optimal Design of Trusses for Overall Stability," *Computers and Structures*, Vol. 53, No. 5, 1994, pp. 1133–1138.

[8]Khot, N. S., "Kamat MP. Minimum Weight Design of Truss Structures with Geometric Nonlinear Behavior," *AIAA Journal*, Vol. 23, No. 1, 1985, pp. 139–144.

[9]Kamat, M. P., and Raungasilasingha, P., "Optimization of Space Truss Against Instability Using Design Sensitivity Derivatives," *Engineering Optimization*, Vol. 8, No. 2, 1985, pp. 177–188.

[10]Kamat, M. P., Khot, N. S., and Watson, L. T., "On Optimizing Frame Type Structures in Nonlinear Response," *Computer Methods for Nonlinear Solids and Structural Mechanics*, Vol. 54, Applied Mechanics Div., American Society of Mechanical Engineers, New York, 1983, pp. 111–119.

[11]Kamat, M. P., "Optimization of Shallow Arches Against Instability Using Sensitivity Derivatives," *Finite Elements in Analysis and Design*, Vol. 3, No. 4, 1987, pp. 277–284.

[12]Park, J. S., and Choi, K. K., "Optimal Sensitivity Analysis of Critical Load Factor for Nonlinear Structural Systems," *Computers and Structures*, Vol. 36, No. 5, 1990, pp. 823–838.

[13]Zienkiewicz, O. C., "Incremental Displacements in Nonlinear Problems," *International Journal for Numerical Methods in Engineering*, Vol. 3, No. 4, 1971, pp. 587–592.

[14]Haisler, W. E., Stricklin, J. A., and Key, J. E., "Incrementation in Nonlinear Structural Analysis by Self-Correcting Method," *International Journal for Numerical Methods in Engineering*, Vol. 11, No. 1, 1977, pp. 3–10.

[15]Batoz, J. L., and Dhatt, G., "Incremental Displacement Algorithms for Nonlinear Problems," *International Journal for Numerical Methods in Engineering*, Vol. 14, 1979, pp. 1262–1267.

[16]Sedaghati, R., and Tabarrok, B., "Optimum Design of Truss Structures Undergoing Large Deflections Subject to a System Stability Constraint," *International Journal of Numerical Methods in Engineering*, Vol. 48, No. 3, 2000, pp. 421–434.

[17]Sedaghati, R., Tabarrok, B., and Suleman, A., "Structural Design Optimization of Nonlinear Symmetric Structures Using the Group Theoretic Approach," *AIAA Journal*, Vol. 39, No. 8, 2001, pp. 1593–1599.

[18]Sedaghati, R., Suleman, A., and Tabarrok, B., "Optimum Design of Frame Structures Undergoing Large Deflections Against System Instability," *Proceedings of the First MIT Conference on Computational Fluid and Solid Mechanics*, Vol. 1, edited by K. J. Bathe, Massachusetts Inst. of Technology, Cambridge, MA, 2001, pp. 725–728.

[19]Valido, A. J., and Cardoso, J. B., "Geometrically Nonlinear Composite Beam Structures: Design Sensitivity Analysis," *Journal of Engineering Optimization*, Vol. 35, No. 5, 2003, pp. 531–551.

[20]Valido, A. J., and Cardoso, J. B., "Geometrically Nonlinear Composite Beam Structures: Optimal Design," *Journal of Engineering Optimization*, Vol. 35, No. 5, 2003, pp. 553–560.

[21]Haftka, R. T., and Gürdal, Z., *Elements of Structural Optimization*, Kluwer Academic, Dordrecht, The Netherlands, 1992, Chap. 7.

[22]Mroz, Z., and Haftka, R. T., "Design Sensitivity Analysis of Non-Linear Structures in Regular and Critical Sates," *International Journal of Solids and Structures*, Vol. 31, No. 15, 1994, pp. 2071–2098.

[23]Bathe, K. J., *Finite Element Procedures*, Prentice–Hall, Upper Saddle River, NJ, 1996, Chap. 6.

[24]Belytschko, T., and Hseih, J., "Nonlinear Transient Finite Element Analysis with Convected Co-Ordinates," *International Journal for Numerical Methods in Engineering*, Vol. 7, No. 3, 1973, pp. 255–271.

[25]Rankin, C. C., and Brogan, F. A., "An Element Independent Co-Rotational Procedure for the Treatment of Large Rotations," *Journal of Pressure Vessel Technology*, Vol. 108, No. 2, 1986, pp. 165–174.

[26]Chang, S. C., and Chen, J. J., "Effectiveness of Linear Bifurcation Analysis for Predicting the Nonlinear Stability Limits of Structures," *International Journal for Numerical Methods in Engineering*, Vol. 23, No. 5, 1986, pp. 831–846.

[27]Powell, M. J. D., "A Fast Algorithm for Nonlinearly Constrained Optimization Calculations," *Proceedings of the 1977 Dundee Conference on Numerical Analysis*, Vol. 630, Lecture Notes in Mathematics, edited by G. A. Watson, Springer-Verlag, Berlin, 1978, pp. 144–157.

[28]Coleman, T., Branch, M. A., and Grace, A., *Optimization Toolbox-For Use with Matlab*, User's Guides, Ver. 2, MathWorks, Inc., Natick, MA, 1999.

A. Messac
Associate Editor